European Congress on Computational Methods in Applied Sciences and Engineering
ECCOMAS Computational Fluid Dynamics Conference 2001
Swansea, Wales, UK, 4-7 September 2001

COMPUTATION OF COMPRESSIBLE, IMMISCIBLE WATER-AIR FLOWS UNDER THE ACTION OF GRAVITY

Barry Koren, Mervyn R. Lewis

CWI, P.O. Box 94079, 1090 GB Amsterdam, The Netherlands
Barry.Koren@cwi.nl, Mervyn.Lewis@cwi.nl
webpage: http://www.cwi.nl/

Key words: non-homogeneous hyperbolic system, free-surfaces, linearized Godunov scheme, level-set method, ghost-fluid method, splitting method

Abstract. *The present work concerns the numerical simulation of inviscid, compressible and immiscible liquid-gas (water-air) flows in a gravitational field. The flows are described by the Euler equations of fluid dynamics with a source term due to gravity. The effects of this source term are analyzed. The specific form of the source term allows an elegant numerical splitting technique. Numerical results are presented for a tube filled with water and air. The water-air interface is captured using a ghost-fluid algorithm. For computing the separate water and air fluxes a linearized Godunov scheme is applied. For an accurate distinction between water and air a level-set technique is used.*

1 INTRODUCTION

The motivation for this research is an interest in developing a new approach for computing flows which are partially bounded by a freely moving surface. As an example of such flows one may think of water flows around ship hulls with surface wave making. In this case, the solution of the free-surface problem may consist of the solution of the Navier-Stokes equations on the interior of some domain coupled with the determination of the location of the freely moving boundary. Over the last few decades a wealth of numerical techniques has been devised for problems involving free surfaces.

These techniques can be categorized into *surface-tracking* methods, of which the Marker-And-Cell method [1] and the Volume-Of-fluid method [2] are the most prominent ones, *surface-fitting* methods, see, e.g., [3] and *surface-capturing* methods, see, e.g., [4]. It is generally acknowledged that if the free boundary is smooth, in particular if the surface can be represented by a so-called height function, surface-fitting methods are unsurpassed in accuracy and robustness. This is the reason that surface-fitting methods have received much attention from the ship-hydrodynamics community. A major difficulty with surface-tracking and surface-fitting methods occurs when the free surface forms a singularity or when a topological change takes place. These aspects increase the complexity of the method, in case of surface tracking, or even render the method useless, as is the case with surface fitting. A method which is capable of dealing with singularities and/or topological changes is preferable. The capturing method offers a more flexible approach, at least theoretically, through solving the flow equations on both sides of the interface in such a manner that the solution (automatically) satisfies the proper interface conditions. However, this method is also not without drawbacks, see for instance [5] on the phenomenon of pressure oscillations in multicomponent Euler flows. Furthermore, capturing methods tend to smear large density gradients over several cells. We will advocate a special capturing method, called the *ghost-fluid method*, that will keep the density jump across the interface sharp.

In the current paper we consider the computation of inviscid, compressible and immiscible liquid-gas (water-air) flows in a gravitational field. The dynamics of both fluids is described by the Euler equations. Through the assumption of compressibility the gravity force enters the equations as a source term, resulting in a non-homogeneous hyperbolic system. The effects of this non-homogeneity will be investigated, which will lead to an efficient way of implementing the source term into the numerical scheme. All this will be demonstrated on a 1D model problem.

2 EQUATIONS OF MOTION

2.1 Fluid motion

Our prime interest is the case in which one of the fluids is a liquid (e.g., water) and the other a gas (e.g., air). The existence of both fluids in one domain allows a stable equilibrium in which the heavier fluid, water, is underlying the lighter fluid, air. The

fluids are separated by the free surface. Across this interface the density is discontinuous. It is this discontinuity which is generally not well represented on a fixed grid. Our aim is to develop a method which captures the interface and does not smear the (large) discontinuity in the density across a number of cells.

Throughout the remainder of this paper, for convenience, the investigation is focussed on a model problem with one spatial dimension. One may consider this case as a representative model for more complex water-air flows. Note that the resulting numerical method is easily extended to multiple spatial dimensions. But for now all variables are functions of (x,t) only. This has also the advantage that some nice analytical properties can be obtained.

Let us write the 1D system of Euler equations, on some open interval $I \subset \mathbb{R}$, in conservation form, i.e., as

$$\partial_t \mathbf{q}(x,t) + \partial_x \mathbf{f}(\mathbf{q}(x,t)) = \mathbf{Q}\mathbf{q}(x,t), \quad \forall (x,t) \in I \times \mathbb{R}^+, \tag{1}$$

where

$$\mathbf{q}(x,t) = \begin{pmatrix} \rho \\ \rho u \end{pmatrix}, \quad \mathbf{f}(\mathbf{q}(x,t)) = \begin{pmatrix} \rho u \\ \rho u^2 + p(\rho) \end{pmatrix}, \quad \mathbf{Q} = \begin{pmatrix} 0 & 0 \\ -\mathrm{Fr}^{-2} & 0 \end{pmatrix}. \tag{2}$$

The vector $\mathbf{q}(x,t)$, a function from $I \times \mathbb{R}^+$ into Ω, with $\Omega \subset \mathbb{R}^2$, contains the conserved quantities and the function $\mathbf{f} : \Omega \to \mathbb{R}^2, \mathbf{f} \in C^1(\Omega)$, is called the flux function. $\mathbf{Q}$ is the matrix due to the presence of the gravity force.

The variables x and t are space and time, and ρ, u, p are the density, velocity and pressure. The parameter $\mathrm{Fr} \equiv \frac{U}{\sqrt{gL}}$ is the Froude number, U and L being a characteristic speed and length, and g the acceleration of gravity. The system of equations (1) describes the conservation of mass and momentum for both fluids. The distinction between the two types of fluid is made in the way the system is balanced by an equation of state.

In this paper Tait's equation of state [6] has been adopted for this purpose. This equation has the form

$$\frac{p + Bp_0}{p_0(1+B)} = \left(\frac{\rho}{\rho_0}\right)^{\gamma}, \tag{3}$$

where B, ρ_0 and γ are constants depending on the type of fluid and p_0 is the reference pressure for both fluids. The index 0 refers to some characteristic reference state. Since shock waves have been excluded the only discontinuity in the solution will occur across the interface. Also cavitation is not included in this model.

2.2 Interface motion

Now that the governing equations of motion for the fluids have been established, it remains to specify the location of the free surface. A *level-set method* has been selected for this purpose. See, for instance, [4] and [7] and the references in there for an introduction to level-set methods. In this paper only a brief description of the level-set method, as

used in this work, will be given. The general idea of level-set methods is that an interface can be represented as a smooth hypersurface $\Gamma(t) \in \mathbb{R}^n$ embedded in a smooth $\mathbb{R}^{n+1}$ dimensional function $\phi(\mathbf{x}, t)$ for which it holds

$$\Gamma(t) = \{\mathbf{x} \in \mathbb{R}^n, t > 0 : \phi(\mathbf{x}, t) = 0\}. \tag{4}$$

Thus the motion of the interface $\Gamma(t)$ is matched with the evolution of a function ϕ. Note that in our 1D model problem the interface $\Gamma(t)$ is reduced to a point on the x-axis. First we will construct the initial value $\phi(x, 0)$. A fairly straightforward way of constructing $\phi(x, 0)$ is to let it be a signed-distance function. This is done through setting

$$\phi(x, 0) = \bar{x}(0) - x, \tag{5}$$

where $\bar{x}(0)$ is the location of the free surface at $t = 0$. Note that $\phi(x, 0)$ does not necessarily have to be a distance function, see, e.g., [7]. Secondly the time evolution of $\phi(x, t)$, and therefore also the interface location, is described by

$$\partial_t \phi(x, t) + u(x, t)\partial_x \phi(x, t) = 0, \quad \forall (x, t) \in I \times \mathbb{R}^+, \tag{6}$$

with $u(x, t)$ the underlying velocity field. Alternatively, this equation can be combined with the mass conservation equation to give

$$\partial_t(\rho\phi) + \partial_x(\rho u\phi) = 0, \quad \forall (x, t) \in I \times \mathbb{R}^+. \tag{7}$$

This equation can be incorporated into (1) which then has a state vector $\mathbf{q}(x, t) = (\rho, \rho u, \rho\phi)^T$ and flux function $\mathbf{f}(\mathbf{q}) = (\rho u, \rho u^2 + p(\rho, \phi), \rho u\phi)^T$. Note that now $p = p(\rho, \phi)$, this is what is referred to as feedback [7].

3 ANALYSIS

In this section some analytical aspects of the 1D model problem will be explored. First the case where the level-set function ϕ has not been incorporated into system (1) will be considered. (Incorporating the level-set function into the system does not alter the results which are obtained below.) The level-set equation results in an additional (linearly degenerate) eigenvalue $\lambda = u$. As stated previously the dynamics of both fluids is governed by system (1), which is closed by the convex equation of state (3). The system of equations is strictly hyperbolic as can be observed from the eigenvalues of the flux Jacobian $\mathbf{f}'(\mathbf{q})$. These are $\lambda_{1,2} = u \pm c$. Note that $\mathbf{Q}$ does not share any of the eigenvalues of the flux Jacobian. Furthermore a closer inspection of $\mathbf{Q}$ reveals that $\dim(\mathcal{N}(\mathbf{Q})) = 1$, where $\mathcal{N}(\mathbf{Q})$ is the null space of $\mathbf{Q}$. This means that at least one quantity is conserved in this system.

3.1 Dispersion analysis

A dispersion analysis of the system is useful in understanding the behaviour of the system. This is important not only from a physical point of view but also from a numerical

point of view, because the discrete system should –ideally– have the same characteristics to accurately approximate the (continuous) solution. Also stability of the numerical scheme largely depends on the wave speeds in the system. By inserting a single Fourier mode with wave number k,

$$\mathbf{q}(x,t) = \hat{\mathbf{q}} e^{i(kx-\omega(k)t)}, \tag{8}$$

into the quasi-linear form of system (1) the following dispersion relation is obtained

$$\omega(k) = k\left(u \pm c\sqrt{1 - i\frac{1}{\mathrm{Fr}^2 kc^2}}\right), \quad i^2 \equiv -1. \tag{9}$$

This relation tells us that the fastest waves in the system travel with the phase velocity

$$v_p = \frac{\omega(k)}{k} = u \pm c\frac{\sqrt{\mathrm{Fr}^2 kc^2}}{2\sqrt[4]{1 + (\mathrm{Fr}^2 kc^2)^2}}. \tag{10}$$

From the phase velocity, it can be concluded that the system is dispersive due to the presence of the gravitational field. Note that for $\mathrm{Fr}^2 \uparrow \infty$ both acoustic modes are recovered. Here, short waves ($k \gg 1$) travel faster than long waves ($k \ll 1$). This effect is dependent on the speed of sound of the medium through which the waves travel. Also, it can be seen from (10) that the long waves travel at a speed

$$v_p \approx u \pm \frac{1}{2}\mathrm{Fr}\sqrt{k}c^2, \tag{11}$$

which, for subcritical flows ($\mathrm{Fr} < 1$), is less than $v_p = u \pm c$, i.e., the speed for short waves. Therefore the stability condition of our explicit time-integration method is satisfied as long as the CFL number $\sigma = \frac{v_p \Delta t}{\Delta x}$, $v_p = u \pm c$ is smaller than 1.

3.2 Homogenization

In dealing with non-homogeneous systems of PDE's a number of different approaches has been developed. For instance in [8] it is shown that by incorporating the source term into the flux function, as opposed to evaluating the source term in some straightforward manner, improvements in both accuracy and convergence rate are accomplished. This result justifies the search for transformations through which the source term can be incorporated into the flux function. In the remainder of this section we will investigate a transformation which does precisely that.

Consider the following change of dependent variables

$$\mathbf{q}(x,t) = \theta(\mathbf{w}(x,t)) \quad \Leftrightarrow \quad \theta(\mathbf{w}(x,t)) = e^{t\mathbf{Q}}\mathbf{w}(x,t), \tag{12}$$

where $\mathbf{w} : I \times \mathbb{R}^+ \to \mathbb{R}^2$ is the vector of the transformed dependent variables. It is important to note that $\det(\theta'(\mathbf{w})) = 1$ which renders the transformation non-singular. Application of (12) to the system (1) changes this into

$$\partial_t \mathbf{w} + \partial_x \mathbf{G}(\mathbf{w},t) = \mathbf{0}, \tag{13}$$

where

$$\mathbf{G}(\mathbf{w},t) = e^{-t\mathbf{Q}}\mathbf{f}(e^{t\mathbf{Q}}\mathbf{w}) \tag{14}$$

represents the transformed flux function. Note that partial differentiation w.r.t. x has no effect on the exponential term. The set of equations (13) is a system of conservation laws with as the conserved quantities $\mathbf{w} = (w_1, w_2)^T$. From an inspection of the flux Jacobian $\mathbf{G}'(\mathbf{w},t)$, it follows that it has

$$\lambda_k = \frac{w_2}{w_1} - t\mathrm{Fr}^{-2} \pm c, \quad \mathbf{r}_k = (w_1, w_2 \pm cw_1)^T, \quad k = 1,2, \tag{15}$$

as eigenvalues and eigenvectors. Because both eigenvalues are real and distinct, (13) is (still) strictly hyperbolic. Also the effect of the source term becomes apparent through the explicit time dependence of the eigenvalues. Finally, it can be shown that (13) possesses the following Riemann invariants in state space

$$\Psi_k = \frac{w_2}{w_1} \mp \frac{2c(w_1)}{\gamma - 1}, \quad k = 1,2. \tag{16}$$

These Riemann invariants are useful for the construction of simple wave solutions of the Riemann problem. This Riemann problem is formed by (13) supplemented with the initial conditions

$$\mathbf{w}(x,0) = \{\mathbf{w} \subset \Omega : \mathbf{w}_l, x < 0, \mathbf{w}_r, x > 0\}, \tag{17}$$

where $\mathbf{w}_l$ and $\mathbf{w}_r$ are constant states.

3.3 Steady-state solution property

It can be easily shown that the stationary solution of (1) must satisfy

$$H = \frac{1}{2}u^2 + \int \frac{\mathrm{d}p}{\rho} + \mathrm{Fr}^{-2}(x - \bar{x}), \tag{18}$$

where $\bar{x}$ denotes the free-surface location, and where H is a constant specified at some reference point. Relation (18) holds for every inviscid barotropic flow. The pressure integral can be evaluated with the use of (3) resulting in

$$\int \frac{\mathrm{d}p}{\rho} = \frac{c(p)^2}{\gamma - 1}, \tag{19}$$

where c is the speed of sound. Note that H is also discontinuous at the free surface.

4 NUMERICAL METHOD

We use the level-set function to locate the interface. The zero of the level-set function denotes the interface, while positive values correspond to one fluid and negative values correspond to the other fluid. As mentioned before the discretization of the level-set

equation can be done independent of the two sets of Euler equations. This has the advantage that this equation can be discretized through a discretization different from the one used for the system of Euler equations. Many discretizations have been explored for the Hamilton-Jacobi equation which the level-set equation is, see [9]. In [9], Hamilton-Jacobi-type equations are solved by using techniques common for hyperbolic conservation laws. In the present work equation (6) is discretized as follows :

$$\phi_i^{n+1} = \phi_i^n - \lambda \frac{u_i^n + |u_i^n|}{2}(\phi_i^n - \phi_{i-1}^n) - \lambda \frac{u_i^n - |u_i^n|}{2}(\phi_{i+1}^n - \phi_i^n), \tag{20}$$

where $\lambda = \frac{\Delta t}{\Delta x}$. The discretization of the system of Euler equations is obtained through a first-order finite-volume discretization, which, omitting the source term, reads

$$\mathbf{q}_i^{n+1} = \mathbf{q}_i^n - \lambda(\mathbf{F}(\mathbf{q}_i^n, \mathbf{q}_{i+1}^n) - \mathbf{F}(\mathbf{q}_{i-1}^n, \mathbf{q}_i^n)). \tag{21}$$

The numerical flux function $\mathbf{F}$ is calculated using the *linearized Godunov* scheme. Details of this scheme can be found in [10].

The source term in the Euler equations is dealt with in the following manner. Transformation (12) has the following important property. For $t \downarrow 0$, the solution of (13) converges to the solution of (1) with $\mathbf{Q} = 0$. This property inspired us to a two-stage solution algorithm for the non-homogeneous system, in which we do the following per time step:

1. For a time step Δt, solve (1) with $\mathbf{Q} = \mathbf{0}$. This can be done with one's own preferred time integrator.

2. Multiply the solution $\mathbf{q}$ obtained from step 1 with $\mathbf{I} + \Delta t\mathbf{Q}$. Here the property that $\mathbf{Q}$ is nilpotent of index 2 is exploited.

This procedure may be categorized as a splitting method [11]. However, it is not a standard splitting method. Per time step, it requires the solution of a single initial-boundary value problem only, as opposed to the two initial-boundary-value problems that need to be solved in standard splitting methods.

The water-air interface is captured using the *ghost-fluid* method [12]. The method essentially works as follows. Given some level-set function, the computational domain is divided into two separate domains for the two fluids. To calculate the solution at the new time level, so-called ghost cells are defined in the computational domain. As the ghost cells we define those cells in which there is a material interface (i.e., a zero of the level-set function). We consider these cells in an ambiguous way, i.e., as fully filled with water and – also– as fully filled with air. Then, across the two walls of a ghost cell both water and air fluxes are computed. On the basis of the difference between the two fictitious (ghost) water fluxes, the fictitious (ghost) water solution in the interface cell is updated. The (ghost) air solution is updated in a similar fashion. Expressed in (u, p)-variables, these

two new ghost solutions will probably not differ very much, particularly not the water and air velocities. Due to their (density-dependent) dependence on gravity, the water and air ghost pressures will differ more strongly. To remove the solution ambiguity in the ghost cells, we propose the following. From the updated level-set solution, the volume-of-fluid fraction α in the ghost cell can be computed. Then, the solution in the ghost cell is made unique with

$$\begin{pmatrix} u \\ p \end{pmatrix} = \alpha \begin{pmatrix} u_w \\ p_w \end{pmatrix} + (1-\alpha) \begin{pmatrix} u_a \\ p_a \end{pmatrix}. \tag{22}$$

There are no physical or mathematical arguments for applying this weighting, other choices are possible. For details about this approach, particularly about the computation of the ghost fluxes, we refer to [13].

5 NUMERICAL RESULTS

The numerical test case considered in this paper is the steady-state solution of (1) on the interval $I = \{x : x \in [0,1]\}$ for the initial solution

$$u(x,0) = 0, \quad p(x,0) = 1, \quad \forall x \in I, \tag{23}$$

with the free surface initially set at $\bar{x}(0) = 0.5$, for $\mathrm{Fr} = 0.5$, $\rho_w(x,0) = 1$ and $\rho_a(x,0) = 0.001$. The boundary conditions imposed are $u(0,t) = 0$ and $p(1,t) = 1$. So, at $x = 0$ the tube is closed and at $x = 1$ it is open. For the exact analytical solution it holds $u(x,t) = 0$. A very good approximation for the exact pressure at the bottom of the tube ($x = 0$) is

$$p(x=0) = p(x=1) + \frac{(\rho_a)_{init}(l_a)_{init} + (\rho_w)_{init}(l_w)_{init}}{\mathrm{Fr}^2}, \tag{24}$$

where $(l_a)_{init}$ and $(l_w)_{init}$ are the lengths of the initial air and water columns, respectively. Note that for the initial solution chosen, (24) gives the exact bottom pressure value up to and including the third decimal digit: $p(x=0) = 3.002$. Integration of the hydrostatic pressure equation $\frac{\mathrm{d}p}{\mathrm{d}x} = -\mathrm{F}r^{-2}\rho(p)$, with $\rho(p)$ given by (3), yields for water and air, respectively,

$$p_w(x) = \left(\frac{-(\rho_0)_w}{\mathrm{Fr}^2 (p_0(1+B))^{1/\gamma_w}} \frac{\gamma_w - 1}{\gamma_w} x + (p(x=0) + Bp_0)^{\frac{\gamma_w - 1}{\gamma_w}} \right)^{\frac{\gamma_w}{\gamma_w - 1}} - Bp_0, \tag{25}$$

$$p_a(x) = \left(\frac{-(\rho_0)_a}{\mathrm{Fr}^2 (p_0)^{1/\gamma_a}} \frac{\gamma_a - 1}{\gamma_a} (x-1) + (p(x=1))^{\frac{\gamma_a - 1}{\gamma_a}} \right)^{\frac{\gamma_a}{\gamma_a - 1}}. \tag{26}$$

Equating both pressure distributions yields the location of the free surface $\bar{x}$. For the exact values at hand, this means: $\bar{x}_{exact} = 0.49998$. Knowing these exact velocity and pressure distributions, the solution errors can be calculated. The method as proposed in this paper is tested on three different grids, viz. with $\Delta x = 1/40, 1/80$ and $1/160$. The distributions of the pressure and velocity are plotted in figures 1 and 2. (Note that

$(\Delta x)^{-1}$	$\frac{\Delta \bar{x}}{\Delta x}$
40	-9.56×10^{-3}
80	-12.32×10^{-3}
160	-16.80×10^{-3}

Table 1: Relative error in free-surface location.

figure 2 also represents the error in the velocity distribution.) The distribution of the pressure error $\Delta p = p_{num} - p_{exact}$ is plotted in figure 3. Inspection of the pressure-error distributions indicates that the pressure in pure water, and in the interface cell is resolved with first-order accuracy. Also notice the perfect first-order accuracy behaviour of the velocity. For each of the three numerical solutions, table 1 still gives the relative error in the location of the free surface, $\frac{\Delta \bar{x}}{\Delta x} = \frac{\bar{x}_{num} - \bar{x}_{exact}}{\Delta x}$, with $\bar{x}_{exact} = 0.49998$. The free-surface location for the numerical solutions, $\bar{x}_{num} = \bar{x}_{\phi=0}$, has been determined by linear interpolation of the discrete values found. Its order of accuracy seems to converge to $\frac{1}{2}$. Finally, figure 4 shows the distribution of the bulk density on the different grids. The bulk density is defined according to (22). These figures reveal that the large density jump is confined to one cell.

6 CONCLUSIONS

In this paper we have computed the steady-state solution of a flow in a 1D tube, open at one side and containing two immiscible fluids, water and air. Most delicate feature in this problem is the water-air interface with its large density jump ($\rho_w/\rho_a = 1000$). Our computational method, built up out of numerical ingredients such as a level-set technique, a finite-volume discretization, a linearized Godunov scheme, a ghost-fluid approach and a splitting technique for the source term, appears to work fine. Applying first-order accurate state interpolation in the approximate Riemann solver, it yields first-order velocity and pressure accuracy in all finite volumes filled with water and also in the finite volume with the interface. The minor solution wiggle near the interface nicely converges to zero at an $O(h)$ rate. Most important: our computational method does not smear the jump in the density; the large density jump is captured within one cell. Of possible interest for future research is the fact that the source term leads to characteristics which are curved in the (x,t)-plane.

ACKNOWLEDGEMENT

This work was supported by the Netherlands Technology Foundation STW, applied science division of NWO and the technology programme of the Ministry of Economic Affairs.

REFERENCES

[1] F.H. Harlow and J.E. Welch, Numerical calculation of time-dependent viscous incompressible flow of fluid with free surface, *Phys. of Fluids*, **8**, 2182-2189, 1965.

[2] C.W. Hirt and B.D. Nichols, Volume of fluid (VOF) method for the dynamics of free boundaries, *J. Comput. Phys.*, **39**, 201-225, 1981.

[3] E.H. van Brummelen, B. Koren and H.C. Raven, Efficient numerical solution of steady free-surface Navier-Stokes flow, *Report MAS-R0103*, CWI, Amsterdam, 2001.

[4] W. Mulder, S. Osher and J.A. Sethian, Computing interface motion in compressible gas dynamics, *J. Comput. Phys.*, **100**, 209-228, 1992.

[5] S. Karni, Multicomponent flow calculations by a consistent primitive algorithm, *J. Comput. Phys.*, **112**, 31-43, 1994.

[6] G.K. Batchelor, *An Introduction to Fluid Dynamics*, Cambridge University Press, Cambridge, 1983.

[7] B. Koren and A.C.J. Venis, A fed back level-set method for moving material-void interfaces, *J. Comput. Appl. Math.*, **101**, 131-152, 1999.

[8] B. Koren, *A robust upwind discretization method for advection, diffusion and source terms*, in: C.B. Vreugdenhil and B. Koren, eds., Numerical Methods for Advection-Diffusion Problems, Notes on Numerical Fluid Mechanics, **45**, 117-138, Vieweg, Braunschweig, 1993.

[9] S. Osher and J.A. Sethian, Fronts propagating with curvature-dependent speed: algorithms based on Hamilton-Jacobi formulations, *J. Comput. Phys.*, **79**, 12-49, 1988.

[10] B. Koren, M.R. Lewis, E.H. van Brummelen and B. van Leer, Godunov and level-set approaches for two-fluid flow computations, *Report MAS-R01xx*, CWI, Amsterdam (in preparation).

[11] G. Strang, On the construction and comparison of difference schemes, *SIAM J. Numer. Anal.*, **5**, 506-517, 1968.

[12] R.P. Fedkiw, T. Aslam, B. Merriman and S. Osher, A non-oscillatory Eulerian approach to interfaces in multimaterial flows, *J. Comput. Phys.*, **152**, 457-492, 1999.

[13] B. Koren and M.R. Lewis, Computing liquid-gas flows under the action of gravity, *Report MAS-R01yy*, CWI, Amsterdam (in preparation).

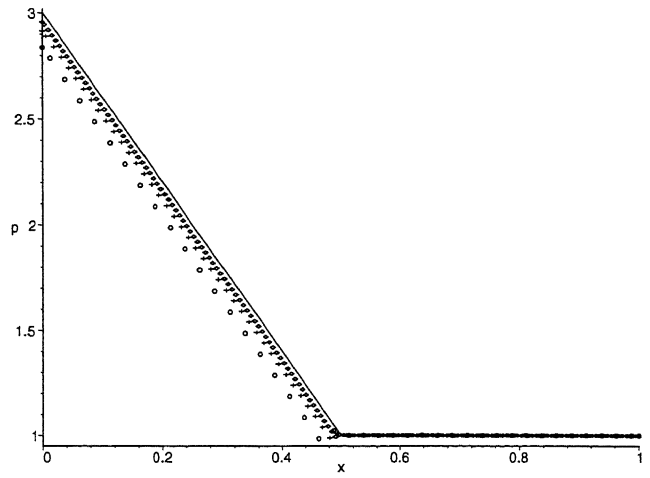

Figure 1: Pressure distribution for grids with $\Delta x = \frac{1}{40}, \frac{1}{80}$ and $\frac{1}{160}$ ($\circ, +$ and $\Diamond$, respectively), and exact (—).

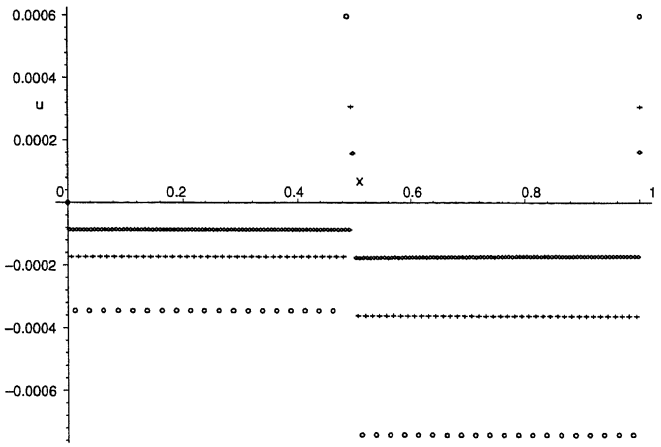

Figure 2: Velocity distribution for grids with $\Delta x = \frac{1}{40}, \frac{1}{80}$ and $\frac{1}{160}$ ($\circ, +$ and $\Diamond$, respectively).

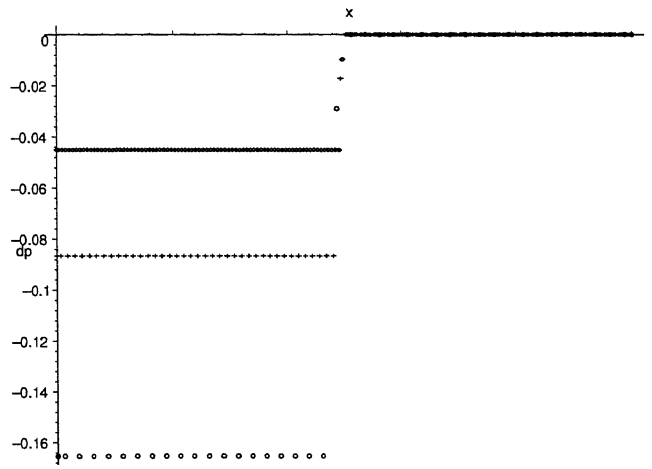

Figure 3: Pressure-error distribution for grids with $\Delta x = \frac{1}{40}, \frac{1}{80}$ and $\frac{1}{160}$ ($\circ, +$ and $\Diamond$, respectively).

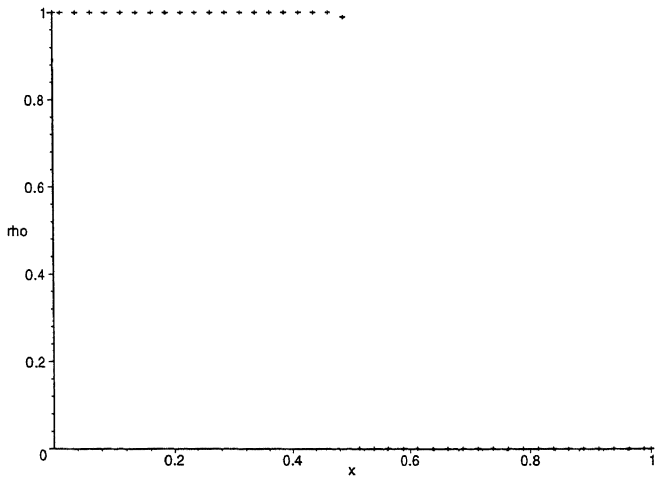

a. $\Delta x = \frac{1}{40}$

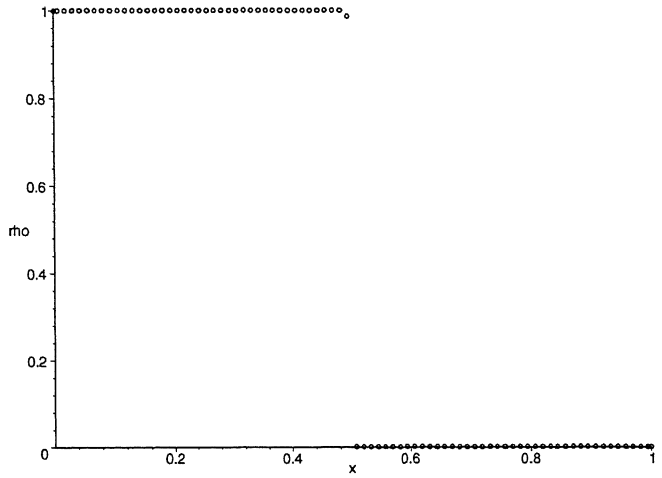

b. $\Delta x = \frac{1}{80}$

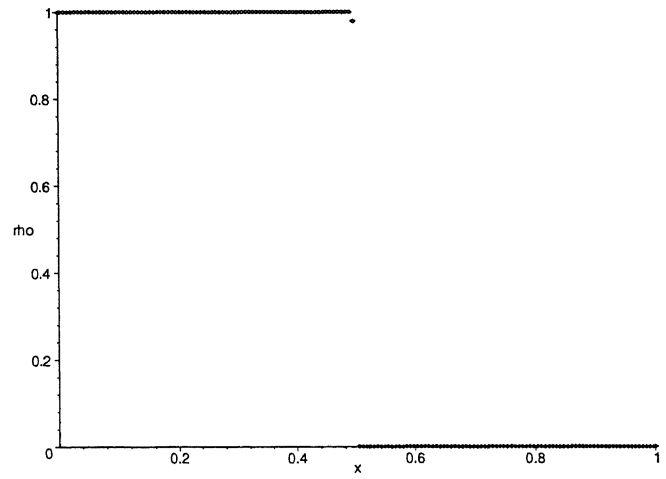

c. $\Delta x = \frac{1}{160}$

Figure 4: Bulk-density distributions for grids with $\Delta x = \frac{1}{40}, \frac{1}{80}$ and $\frac{1}{160}$.